© 2017. Published by The Company of Biologists Ltd | Journal of Cell Science (2017) 130, 2833-2842 doi:10.1242/jcs.202226

RESEARCH ARTICLE

Nestin contributes to skeletal muscle homeostasis and regeneration

Julia Lindqvist[1,2,*], Elin Torvaldson[1,2,*], Josef Gullmets[1,2,3], Henok Karvonen[1,2], Andras Nagy[4], Pekka Taimen[3] and John E. Eriksson[1,2,‡]

ABSTRACT

Nestin, a member of the cytoskeletal family of intermediate filaments, regulates the onset of myogenic differentiation through bidirectional signaling with the kinase Cdk5. Here, we show that these effects are also reflected at the organism level, as there is a loss of skeletal muscle mass in nestin$^{-/-}$ (NesKO) mice, reflected as reduced lean (muscle) mass in the mice. Further examination of muscles in male mice revealed that these effects stemmed from nestin-deficient muscles being more prone to spontaneous regeneration. When the regeneration capacity of the compromised NesKO muscle was tested by muscle injury experiments, a significant healing delay was observed. NesKO satellite cells showed delayed proliferation kinetics in conjunction with an elevation in p35 (encoded by *Cdk5r1*) levels and Cdk5 activity. These results reveal that nestin deficiency generates a spontaneous regenerative phenotype in skeletal muscle that relates to a disturbed proliferation cycle that is associated with uncontrolled Cdk5 activity.

KEY WORDS: Intermediate filament, Nestin, Cdk5, Muscle, Regeneration, Differentiation

INTRODUCTION

Intermediate filament proteins (IFs) are part of the cytoskeleton that provides mechanical stability to the cell. In addition, they are crucial regulators of cell signaling and contribute to several important cellular functions (Gruenbaum and Aebi, 2014; Hyder et al., 2011). Through their association with organelles, structural proteins and signaling executors, IFs are necessary components of the signaling pathways that drive cell migration, adhesion, proliferation, differentiation and death. IFs have the ability to spontaneously form homo- or hetero-polymers, which are fused into long filamentous structures that are constantly remodeled according to the needs of the cell.

The use of genetically engineered mice have revealed essential structural functions for major muscle IFs, such as for desmin, the lack of which disturbs sarcomeres as well as organelle positioning in muscle (Li et al., 1996; Milner et al., 1996, 2000). In addition, the knockout or mutation of the IFs lamin A/C (Kubben et al., 2011; Sullivan et al., 1999), synemin α and β (García-Pelagio et al., 2015; Li et al., 2014) and keratin 19 (Stone et al., 2007) hamper proper myoblast function. A multitude of myopathic desmin and lamin A/C mutations have been identified in human patients, affecting both skeletal and cardiac muscle (Carboni et al., 2013; Goldfarb and Dalakas, 2009; Worman et al., 2009). Different types of muscle injuries are common in all age groups, including myopathies and externally induced injures. Such muscular conditions effect the patient's quality of life negatively and are costly to society, as they require extensive rehabilitation. Severe muscle injury is characterized by a regenerative condition that leads to the activation of muscle stem cells. Prolonged regeneration or inflammation may eventually lead to fibrosis, which severely hampers muscle function. During muscle regeneration, the differentiation of myoblasts, re-innervation of muscle and vascularization, all contribute to healing of the injured site (Ciciliot and Schiaffino, 2010). These physiological processes are not completely characterized, and basic research is therefore of great importance.

The IF protein nestin has received much attention as a progenitor cell marker (Wiese et al., 2004), particularly in the developing central nervous system, where it was first discovered (Hockfield and McKay, 1985). In contrast to many other IFs, nestin has a remarkably short N-terminus, which hinders its self-polymerization; instead, nestin forms heteropolymers with other IFs, such as vimentin and desmin (Sjöberg et al., 1994b; Steinert et al., 1999). Nestin expression is induced during development of the central nervous system and skeletal muscle (Sejersen and Lendahl, 1993). In mice, nestin is expressed during muscle development in the early limb bud and its expression sustains in muscle until birth, after which nestin is downregulated (Carlsson et al., 1999; Sejersen and Lendahl, 1993; Wroblewski et al., 1997). In the adult myofibers, nestin expression is limited to the neuromuscular and myotendinous junctions (Carlsson et al., 1999; Vaittinen et al., 1999). Nestin protein is also expressed in the proliferating progeny of satellite cells, the myoblasts, and transiently in differentiating myotubes (Sahlgren et al., 2003).

Our previous studies show that nestin regulates the differentiation of myogenic precursor cells (Pallari et al., 2011; Sahlgren et al., 2003). The downregulation of nestin in myoblasts was found to increase the differentiation rate through regulation of cyclin-dependent kinase 5 (Cdk5) (Pallari et al., 2011). A bi-directional interplay between nestin and Cdk5 has also been described in apoptotic neuronal progenitor cells (Sahlgren et al., 2006). Studies in mice lacking nestin have in turn shown that nestin has an important role in the development and maintenance of neuromuscular synapses through regulation of appropriate Cdk5 activation (Mohseni et al., 2011; Yang et al., 2011). Upon muscle injury, nestin expression is upregulated in differentiating myoblasts

[1]Cell Biology, Biosciences, Faculty of Science and Engineering, Åbo Akademi University, Turku, 20520, Finland. [2]Turku Centre for Biotechnology, University of Turku and Åbo Akademi University, 20520, Turku, Finland. [3]Department of Pathology, University of Turku and Turku University Hospital, 20520 Turku, Finland. [4]Lunenfeld-Tanenbaum Research Institute, Mount Sinai Hospital, Toronto, M5G 1X5, Canada.
*These authors contributed equally to this work

‡Author for correspondence (john.eriksson@abo.fi)

E.T., 0000-0002-7175-6396; J.G., 0000-0003-2466-7574; P.T., 0000-0001-8849-4604; J.E.E., 0000-0002-1570-7725

Received 16 February 2017; Accepted 12 July 2017

Journal of Cell Science

Journal of Cell Science (2017) 130, 2833-2842 doi:10.1242/jcs.202226

and regenerating myotubes (Vaittinen et al., 2001). Nestin is also upregulated in regenerating myofibers in Duchenne–Becker muscular dystrophy and myositis (Sjöberg et al., 1994a).

While the accumulated data indicate that nestin plays a part in myoblast functions of both healthy and diseased muscle, we employed nestin-knockout mice (Mohseni et al., 2011) to examine how nestin deficiency affects muscle homeostasis under normal conditions and during regeneration *in vivo*. Our results show that nestin deficiency generates a spontaneous regenerative phenotype in skeletal muscle that relates to a disturbed proliferation cycle.

RESULTS

Mice lacking nestin weigh less and have less muscle mass

In this work, we utilized nestin$^{-/-}$ (NesKO) mice to make a comprehensive study of the structure and function of nestin-deficient skeletal muscle. First, the body composition of the mice was analyzed. When NesKO male mice were weighed at different ages, we found that these mice consistently weighed less than the wild-type (WT) counterparts at the age of 3 months (Fig. 1A), a difference that was less obvious in younger mice (data not shown). No difference in food consumption and spontaneous activity level of the mice was observed (Fig. S1), suggesting that the difference in body weight derives from factors affecting tissue and/or body homeostasis rather than changed behavior. The manifestation of body weight difference became increasingly marked in aged (>15 months old) male mice (Fig. 1B), where the average weight difference increased from less than 1 g in 3-month-old mice to more than 7 g in mice that were >15 months old. To dissect which tissues were affected in the NesKO mice, the fat and lean mass (muscle mass) content of 3-month-old mice was measured with Echo-MRI body composition analysis. Corresponding to the lighter weight of NesKO mice, we found that the average lean mass was significantly decreased in the mutants (Fig. 1C), while the average fat mass was similar in both genotypes (Fig. 1C), demonstrating that the weight loss is specifically related to non-adipose tissues. Aged NesKO males had an even greater difference in lean mass compared to that of WT mice (Fig. 1D). The phenotype is gender-independent, as 3-month-old female mice weighed less, and had less lean mass as with the males (Fig. S2A,B), but for practical reasons, male mice were used for all the following experiments. To confirm the assumption that there was a muscle defect, individual muscles from the hind limbs of 3-month-old male mice of both genotypes were weighed. In agreement with the decreased lean mass content in the whole-body measurements, the hind limb muscles tibialis anterior (TA) and extensor digitorum longus (EDL) were found to be significantly lighter in NesKO mice (Fig. 2A), whereas the soleus muscle did not reveal genotype-dependent weight variations. When myofiber area was measured from the soleus and EDL muscles of WT and NesKO mice, no obvious difference could be observed (Fig. 2B,C), suggesting that myofiber caliber is not affected per se.

NesKO skeletal muscle is characterized by the presence of spontaneously regenerating myofibers

The previous results prompted us to investigate the state of NesKO muscle in greater detail. Muscle samples were collected for histology from several hind limb muscles in order to investigate whether nestin has a role in maintenance of muscle tissue during baseline conditions in adult mice. Although the overall morphology of NesKO myofibers was relatively normal, we found that the number of myofibers with centrally located nuclei (CLN), a

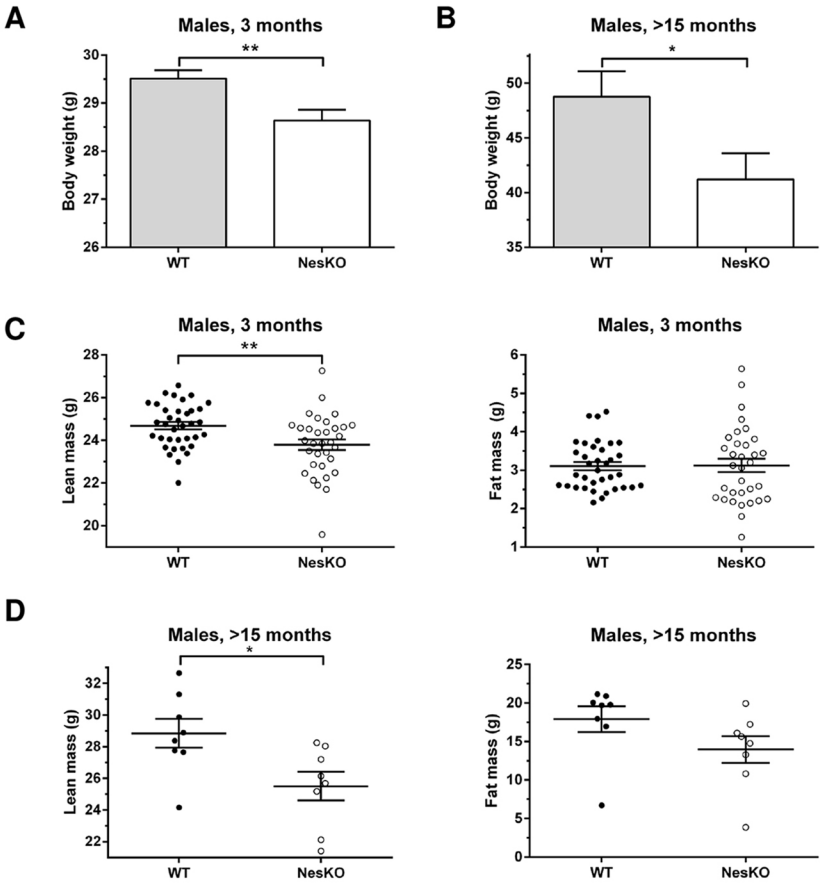

Fig. 1. NesKO mice weigh less and have less lean mass. (A) Body weight of WT and NesKO male mice at 3 months (WT, *n*=75; NesKO, *n*=68; ***P*=0.0027 by Student's *t*-test with Welch's correction). NesKO mice were found to weigh significantly less. (B) Total body weight mean values of WT and NesKO male mice at age >15 months (range 15–17 months; WT, *n*=9; NesKO, *n*=11; **P*=0.0372 by Student's *t*-test with Welch's correction). (C) Body composition of male mice at the age of 3 months. Absolute values of lean (left panel) and fat mass (right panel) in grams are displayed in the scatter plots. In comparison with WT mice (*n*=36), NesKO mice (*n*=33) had significantly less lean mass (***P*=0.0048 by Student's *t*-test with Welch's correction). Average fat mass was not significantly different (WT, *n*=36; NesKO, *n*=33). (D) Body composition measurement of WT and NesKO male mice at age >15 months. Left panel, average lean mass (WT, *n*=8; NesKO, *n*=8; **P*=0.0221 by Student's *t*-test with Welch's correction). Right panel, average fat mass (WT, *n*=8; NesKO, *n*=8; n.s.). Results are mean±s.e.m.

Journal of Cell Science (2017) 130, 2833-2842 doi:10.1242/jcs.202226

A

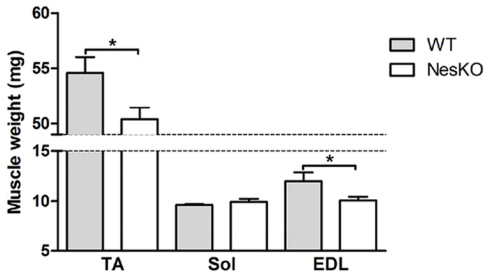

B

Average myofiber size (μm²) ± s.e.m.

	Sol	EDL
WT	1125 ± 110	990.0 ± 31
NesKO	1051 ± 94	1085 ± 39
	n.s. (p>0.05)	n.s. (p>0.05)

C

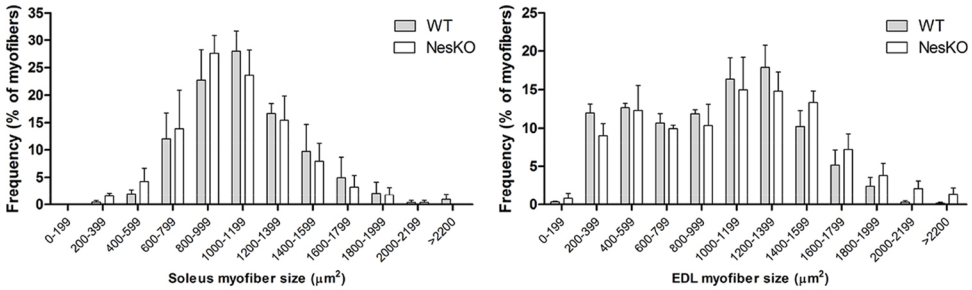

D

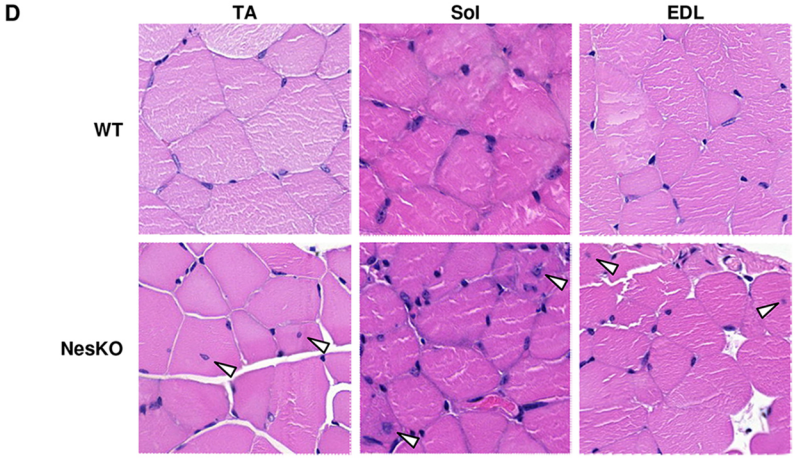

E

Number of myofibers with CLN (average/mm² ± s.e.m.)

	TA	Sol	EDL
WT	1.72 ± 0.4, n=7	2.15 ± 1, n=6	3.95 ± 1.1, n=7
NesKO	3.57 ± 1, n=10	5.25 ± 1.9, n=10	4.41 ± 0.6, n=10
	p=0.025	n.s. (p>0.05)	n.s. (p>0.05)

Fig. 2. NesKO skeletal muscle shows muscle type-specific weight differences and a spontaneous mild regenerative phenotype. (A) Isolated tibialis anterior (TA), soleus (Sol) and extensor digitorum longus (EDL) muscles were isolated and weighed. While the Sol weight did not show a marked difference, both TA and EDL muscles from nestin-null animals weighed significantly less (WT, *n*=4; NesKO, *n*=7; **P*=0.0401 and 0.0391, respectively, by Student's *t*-test with Welch's correction). (B) The average myofiber size from Sol and EDL histological sections does not differ between genotypes. WT, *n*=3, NesKO, *n*=3. More than 250 myofibers from Sol and 500 myofibers from EDL were counted from each mouse. (C) Myofiber size plotted as a frequency distribution for Sol (left panel) and EDL muscles (right panel), respectively. (D) H&E-stained TA, soleus and EDL muscles were investigated for morphological aberrations. White arrowheads mark myofibers with CLN, denoting the presence of degenerating/regenerating myofibers, the occurrence of which tended to be higher in NesKO muscles. H&E images represent tissue of 0.12 mm×0.12 mm in size. (E) The amount of myofibers with CLN was calculated from two muscle sections per mouse. The average amount of CLN per mm² was determined, demonstrating that nestin-null mice tend to have a higher incidence of CLN than WT mice. n represents the number of mice; from each mouse only muscles from the left leg were used. The difference was statistically significant in the TA muscle (*P*=0.0249, Mann–Whitney test). Results are mean±s.e.m.

standard marker for regenerating muscle (Yin et al., 2013), was higher in the NesKO muscles. This was most obvious in the TA and soleus muscles (Fig. 2D,E). The more-obvious effects may reflect the different use of the muscles, as they are typical weight-bearing muscles, or alternatively, differences in fiber type composition. This suggests that, in the absence of nestin, muscle fibers are intrinsically more prone to undergo spontaneous regeneration, a phenotype that is likely to emerge as more severe under specific stressful conditions in specific muscles.

Taken together, these observations point towards an intrinsic defect in nestin-null muscle. As the NesKO muscles weigh less, but contain equally sized myofibers, the results suggest that the mice do not have a myofiber maturation defect that would result in poor myofibers, but simply have less skeletal muscle. This is a phenotype that is also reflected in the whole-body analysis of the animals. As indicated by the fact that there is already an increased number of regenerating myofibers in NesKO mice of a fairly young age, it seems as NesKO mice have underlying problems with muscle homeostasis, the outcome of which is reflected as reduced muscle mass.

NesKO myoblasts have increased Cdk5 kinase activity

Our previous studies have identified nestin as a regulator of the pace and onset of myoblast differentiation through a Cdk5-dependent mechanism (de Thonel et al., 2010; Pallari et al., 2011; Sahlgren et al., 2003). Therefore, it was of interest for us to assess whether the genetic depletion of nestin could affect myoblast differentiation. For this purpose, we employed primary myoblast cultures, which are

Journal of Cell Science (2017) 130, 2833-2842 doi:10.1242/jcs.202226

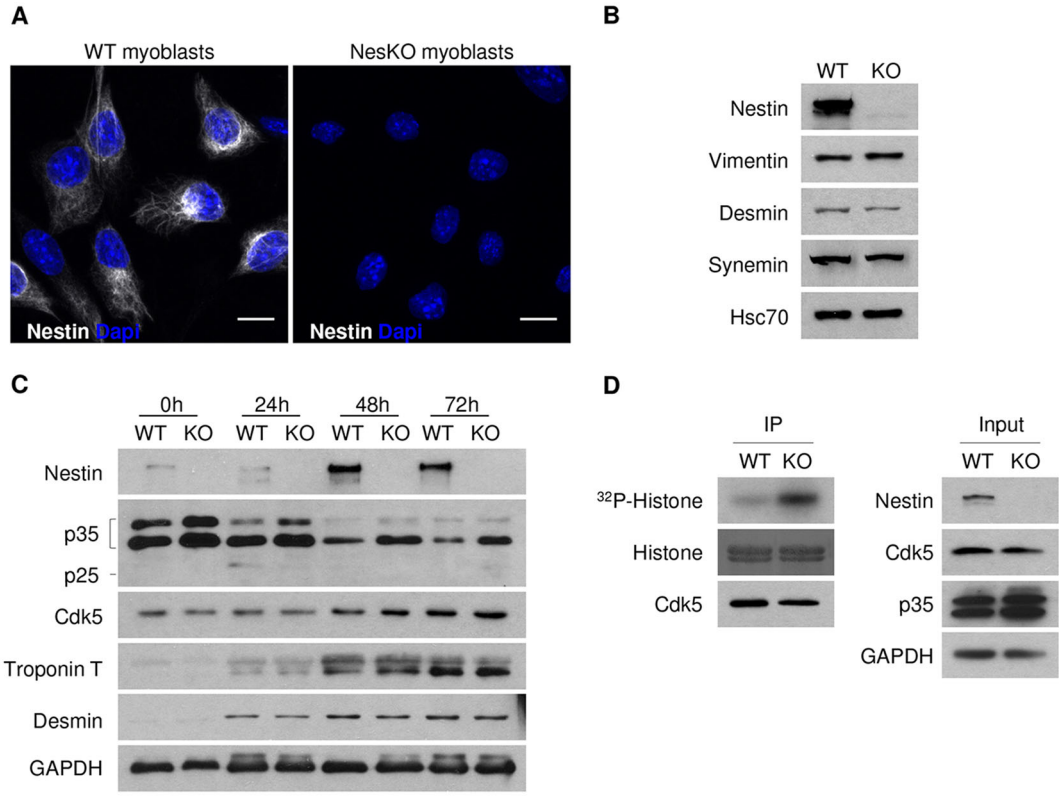

Fig. 3. NesKO myoblast cultures have higher Cdk5 activity, but differentiate at a comparable rate to WT cultures. (A) Myoblasts isolated from WT and NesKO mice were immunolabeled for nestin to demonstrate the absence of nestin in NesKO myoblasts. WT myoblasts exhibited a filamentous nestin labeling in the proliferating cultures. Scale bars: 10 µm. (B) Differentiating WT and NesKO P3 myoblasts were analyzed by western blotting for expression of nestin and other IFs. No recurring differences in the expression levels of other IFs could be detected. (C) Myoblasts were isolated from adult male mice, induced to differentiate, and samples were collected for western blotting at the indicated time points, representing the progress of differentiation. Myoblasts isolated from WT and NesKO mice differentiate equally, as determined by the expression of desmin and troponin T. The protein levels of p35 were, however, increased in NesKO myoblasts. (D) Cdk5 was immunoprecipitated from myoblasts and subjected to activity measurements *in vitro* using histone H1 as a substrate. The [γ-^{32}P]ATP incorporation into histone was considerably increased in nestin-null myoblast cultures, denoting that Cdk5 activity is increased in NesKO myoblasts. The isolation of myoblasts and all subsequent experiments were repeated three times.

prepared by mincing of muscle tissue, resulting in release of a large amount of myogenic cells suitable for producing adequate amounts of samples for biochemical purposes. The primary myoblasts were isolated from adult male mice and immunolabeled and blotted with anti-nestin antibody to demonstrate that the NesKO myoblasts are devoid of nestin (Fig. 3A,B). The primary myoblasts from both genotypes formed myotubes in culture when differentiation was induced. In addition, the protein levels of other muscle IFs were similar between genotypes, not revealing any obvious compensatory expression in NesKO myoblasts (Fig. 3B). Next, several time points (indicated as hours after induction of differentiation) were analyzed through western blotting for the expression of the differentiation markers troponin T and desmin, to study whether nestin ablation affected the pace of primary myoblast differentiation. While in our previous study, we observed an accelerated differentiation along with activation of the Cdk5 pathway after siRNA-mediated nestin depletion in C2C12 cells (Pallari et al., 2011), we could not detect a difference in differentiation kinetics in NesKO primary myoblasts (Fig. 3C). However, we did observe that myoblasts from adult NesKO mice showed markedly increased levels of the Cdk5 activator p35 (encoded by *Cdk5r1*). This was particularly obvious when myoblasts were still in a proliferative state (0 h) and during early stages of differentiation (24 h), that is, when myoblasts have entered the myogenic program but before myotube formation (Fig. 3C). As differentiation proceeded, the overall protein levels of p35 were downregulated progressively in both genotypes. Although p35 levels were elevated in myoblasts from NesKO mice, we did not observe any consistent changes in p25 levels (p25 is the cleaved form of p35), which is seen as a faint band transiently at the 24 h time point in Fig. 3C, between genotypes.

To confirm that the p35 upregulation directly affects Cdk5 kinase activity, Cdk5 was immunoprecipitated from primary myoblasts and used for a kinase activity assay, where Cdk5 phosphorylated histone H1 *in vitro* in the presence of γ-^{32}P-ATP. The results confirmed that Cdk5 activity is dramatically upregulated in nestin-deficient myoblast cultures (Fig. 3D), as already suggested by the increased p35 levels. Hence, there is the distinct possibility that in both proliferating and differentiating myoblasts, nestin balances p35 levels and Cdk5 activity (Mohseni et al., 2011; Pallari et al., 2011). This activation seems to serve a different purpose than amplifying differentiation, which is not surprising, as Cdk5 has many action modes, depending on how it is activated and where it is located (Contreras-Vallejos et al., 2012; Shah and Lahiri, 2014).

NesKO satellite cells show disturbed proliferation

The *Nes* locus has been reported to be active in satellite cells and is considered to characterize the quiescent state of these cells (Day

Journal of Cell Science (2017) 130, 2833-2842 doi:10.1242/jcs.202226

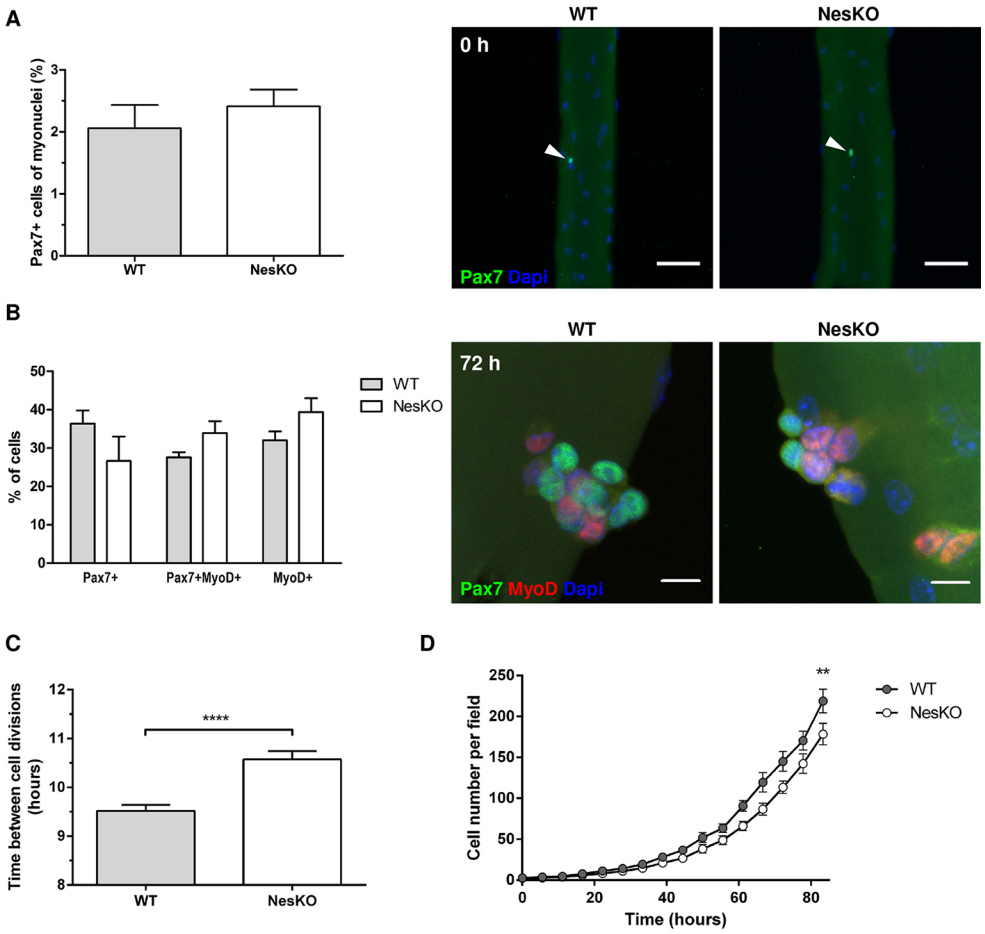

Fig. 4. Satellite cell expansion is affected in the absence of nestin. (A) Intact myofibers were isolated from EDL muscle, and live fibers were fixed immediately. Myofibers were stained for the satellite cell marker Pax7 and the number of Pax7+ cells was calculated. White arrowheads mark Pax7+ cells. Scale bars: 50 µm. Results are visualized as the fraction of Pax7+ cells over the total amount of myonuclei (>2000 myonuclei counted per mouse; n=3 for both WT and NesKO; n.s.). (B) Myofibers isolated from WT and NesKO mice were cultured in floating conditions for 72 h. Myofibers with associated satellite cells were then fixed, and immunolabeled with Pax7 and MyoD antibodies to assess the proportion of cells that have committed to the myogenic lineage (MyoD+). No obvious difference in satellite cell commitment was observed. Scale bars: 10 µm. (C) Single satellite cells emerging from cultured myofibers were manually tracked with Fiji/TrackMate, and the time between satellite cell divisions was calculated (WT, 9.52 h, n=111; NesKO, 10.6 h, n=111; ****P<0.0001 by Student's t-test with Welch's correction). (D) Isolated myofibers were plated on Matrigel-coated dishes, and emerging satellite cells were imaged continuously with the Cell-IQ-imaging platform. The numbers of proliferating satellite cells was calculated at indicated time points with Cell-IQ Analyzer software. The average number of cells per field at 83 h was 219 for WT and 178 for NesKO; **P=0.0054 by Student's t-test, n=3. Results are mean±s.e.m.

et al., 2007). Furthermore, nestin expression has been correlated with proliferation in several non-myogenic cell models (Daniel et al., 2008; Li et al., 2015; Tschaharganeh et al., 2014; Zhao et al., 2014). Therefore, we found it relevant to study the behavior of NesKO muscle stem cells in more detail. To achieve a pure culture model that would still enable us to study the satellite cell behavior in a setting that was as close to the *in vivo* environment as possible, myofiber cultures were utilized as an *in vivo*-like system that allows for long-term live cell imaging. First, to assess whether the absence of nestin influences the overall number of satellite cells under basal conditions, freshly isolated myofibers were fixed immediately after isolation (0 h) and immunolabeled for the satellite cell-specific marker Pax7. No obvious nestin-dependent differences in the amount of Pax7+ satellite cells were observed (Fig. 4A). Next, to characterize satellite cell commitment to the myogenic lineage, myofiber explants were incubated in floating conditions for 72 h, allowing satellite cell activation to occur on top of the fibers, a process that is characterized by the induction of MyoD expression when cells become committed to the myogenic lineage. After 72 h, the live myofibers were fixed, and immunolabeled for Pax7 (a marker for quiescent and activated satellite cells) and MyoD (also known as MyoD1, expressed in committed satellite cells), to assess the commitment and differentiation potential of satellite cells. Quantification of the relative amounts of Pax7+, Pax7+/MyoD+ double-positive and MyoD+ cells showed no consistent change in satellite cell commitment (Fig. 4B).

To address whether the proliferation of satellite cells was affected, myofibers were allowed to attach to Matrigel-coated cell culture dishes for 48 h, after which they were imaged for 96 h via live-cell phase contrast microscopy. In this experimental model, satellite cells migrate out from the fibers and proliferate in their vicinity to then fuse and form new muscle fibers or strengthen the existing fibers (Movie 1). First, we followed the proliferative behavior of individual satellite cells through lineage tracking. When the times between two cell divisions for individual cells were extracted from the data, NesKO satellite cells were revealed to have a doubling time that was 1 h longer (Fig. 4C). These results prompted us to further study the proliferation kinetics of the knockout myoblasts. For this purpose, satellite cell numbers were quantified with Cell-IQ Analyser from comparable image fields and plotted against time, revealing that NesKO satellite cell counts lagged in comparison to WT (Fig. 4D), corresponding well to the lag in doubling time (Fig. 4C).

In summary, our results suggest that knockout of nestin does not alter quiescent satellite cell numbers, their myogenic commitment or the behavior of myoblasts upon a differentiation stimulus as assessed by western blotting. Instead, the myogenic NesKO cells show a delay in their cell proliferation kinetics, which may be coupled to deregulation of Cdk5, the activity of which has been associated with cell cycle exit during myogenic differentiation (Lazaro et al., 1997). The effects on proliferation are, in the end, likely to have consequences during tissue stress and at times of active cell proliferation.

Journal of Cell Science (2017) 130, 2833-2842 doi:10.1242/jcs.202226

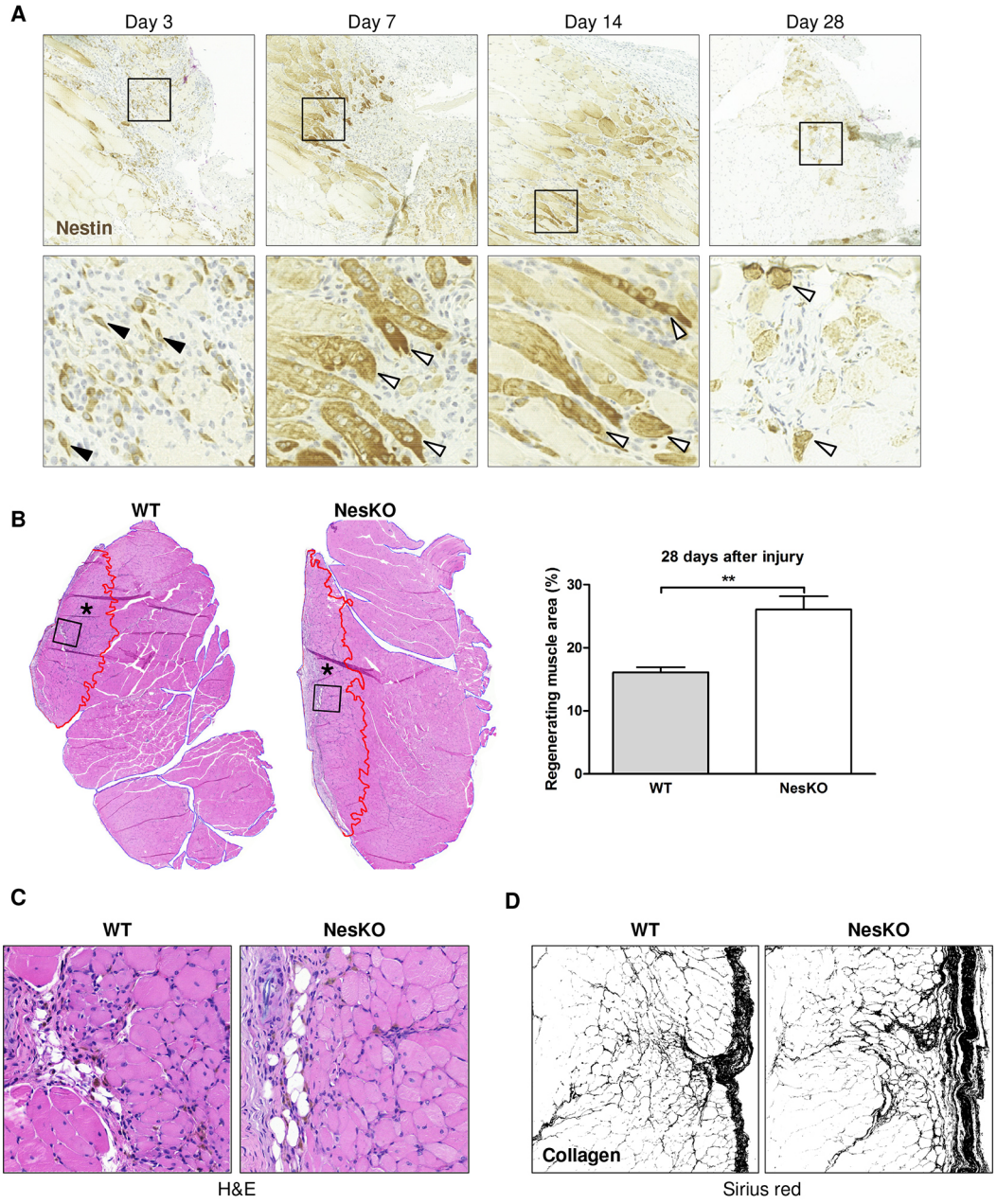

Fig. 5. Muscle regeneration after injury is delayed in NesKO mice. (A) TA muscles of WT mice were injured and samples were collected for paraffin sections at the indicated time points (days after injury). Samples were immunolabeled with anti-nestin antibody, demonstrating the kinetics and localization of nestin expression in healing muscle. Black arrowheads mark single-nucleated myoblasts. White arrowheads mark multinucleated myotubes. Upper images represent tissue of 1 mm×1 mm and inserts below represent tissue of 0.2 mm×0.2 mm in size. (B) WT (n=5) and NesKO (n=5) mice were subjected to muscle injury, and the wound was allowed to heal for 28 days. The regenerating muscle area (defined by the presence of CLN in myofibers) was calculated and compared to the total muscle area, revealing that NesKO mice have a significantly larger area occupied by regenerating myofibers 28 days after injury (WT at 16.10% vs NesKO at 26.06%; **P=0.0023 Student's t-test). The injured area is marked with an asterisk and is outlined in red. Whole muscle sections show representative results for the injured muscle area. Results are mean±s.e.m. (C) H&E-stained samples from the injured muscles areas highlighted by boxes in B were inspected for histological aberrations, but showed no obvious difference, except in the area occupied by regenerating fibers. H&E images represent tissue of 0.3 mm×0.3 mm in size. (D) Fibrotic deposits were studied after injury and Picrosirius Red staining against collagen, through brightfield microscopy. Images were transformed to binary black-and-white images to enhance the visibility of the collagen extracellular matrix (visualized in black). The images represent tissue of 0.5 mm×0.5 mm in size.

Muscle healing after injury is delayed in mice lacking nestin

Next, we wanted to investigate whether the depletion of nestin would affect muscle healing *in vivo*. To this end, a muscle regeneration study was performed in which traumatic muscle injury was mimicked by a transverse incision of the TA muscle of 2-month-old WT and NesKO mice. Using immunohistochemistry, we initially confirmed that nestin is indeed expressed in regenerating WT muscle following injury (Fig. 5A). Nestin-null muscle lacked nestin immunoreactivity, as expected (Fig. S3). During the earliest time points examined (3 days post-injury), nestin was clearly detected in the proliferating WT myoblasts (Fig. 5A). At 7 and 14 days after injury, the newly formed myotubes showed intense nestin reactivity, especially at the tips of the tubes. The expression of nestin was sustained until 28 days post injury, when it

Journal of Cell Science (2017) 130, 2833-2842 doi:10.1242/jcs.202226

could be detected in the still regenerating myofibers (Fig. 5A). Therefore, 28 days after injury was selected as an endpoint for the regeneration study. At this time, the acute phase, characterized by necrosis, inflammation and degeneration, is over, but regeneration is still detectable. Whole muscles were cut in successive parallel planes, and the sections closest to the site of injury were used for quantification of the scar size. The regenerating area was set as the area of scar tissue and regenerating myofibers (determined by the presence of CLN) and compared to the total muscle area. The regenerating area was significantly greater in the NesKO mice, suggesting that nestin is required for normal muscle healing (Fig. 5B). This is in line with the results demonstrating a higher proportion of spontaneous regeneration in uninjured NesKO muscle. While nestin deficiency clearly hampered regenerative capacity, the overall sequence of events in muscle healing seems to be comparable between WT and NesKO (Fig. 5C,D). Taken together, our results show that nestin is required for the maintenance of skeletal muscle physiology and correct muscle healing after injury.

DISCUSSION

We have previously shown that nestin acts as a scaffold for Cdk5 during myogenic differentiation (Pallari et al., 2011; Sahlgren et al., 2003). Owing to this link between nestin and myogenic differentiation, the purpose of the current study was to address the role of nestin in skeletal muscle function and regeneration at the organism level. The study revealed that NesKO mice weigh less and have less lean mass. The detailed analysis of body composition determined that the weight loss is a result of a reduction in muscle mass. Nestin is, however, also expressed in cardiac muscle during development (Kachinsky et al., 1995). Although we did not study this cell type extensively, we could not observe any obvious changes in the histology of the heart. Rather than maturation of individual muscle fibers failing, the muscle defect seems be related to a regeneration problem, as our results showed increased regeneration in NesKO myofibers, and that the situation was further exacerbated upon injury of the muscles. This effect was illustrated by increased presence of CLN in non-injured muscle, and by delayed regeneration of injured muscle. CLN has long been regarded as a marker for regeneration, but there is also growing evidence that proper localization of myonuclei is required for normal muscle function. Consequently, loss of nuclear positioning has been linked to myopathies (Cadot et al., 2015; Folker and Baylies, 2013). Hence, the increased number of CLN we detect in NesKO muscle could be due to increased regeneration or a consequence of a phenotype related to a muscle disorder due to mispositioning of nuclei. While our interpretation is that the observed phenotype is linked to elevated regeneration, the possibility that nestin deficiency could be coupled to nuclear positioning in some other way will require further examination.

Intriguingly, we also found that NesKO satellite cells had slower proliferation kinetics in myofiber explant cultures, although the number of quiescent satellite cells was unaffected. Two key phenomena in literature support the notion that nestin is associated with cell proliferation. Firstly, nestin is known to be expressed in several rapidly expanding cells, such as in many progenitor cell types and in various cancers (Tampaki et al., 2014; Wiese et al., 2004). Secondly, nestin downregulation has been repeatedly shown to negatively affect the cell cycle and proliferation of many cell types (Daniel et al., 2008; Li et al., 2015; Tschaharganeh et al., 2014; Zhao et al., 2014). In light of these observations, it is highly plausible that the regenerative muscle phenotype and delayed muscle healing observed in the NesKO mice would be consequences of the decreased proliferation rate of the satellite cells. It is widely acknowledged that defects in myogenic proliferation, caused by defective satellite cell-associated signaling proteins, contribute to flawed muscle function and regeneration (Shi and Garry, 2006; Yin et al., 2013). While the observed delay in proliferation of the NesKO satellite cells may appear relatively mild during the early phases of satellite cell expansion and as examined in *in vitro* conditions, it may have serious implications for muscle function, durability and homeostasis during times of heavy cell expansion *in vivo*, such as during healing after injury, or regeneration and expansion following physical activity. In this respect, proper satellite cell activation and proliferation are indispensable for the process of muscle maintenance and regeneration.

The results presented in this work support our previously established concept of nestin-mediated regulation of Cdk5 activity, showing that nestin serves as a scaffold for Cdk5 (Sahlgren et al., 2003, 2006; Pallari et al., 2011). Related to the scaffolding role, we have shown that nestin siRNA in C2C12 myoblasts promoted Cdk5 activity through stabilization of the Cdk5 activator p25 (Pallari et al., 2011). Related to these observations, we observed in the primary NesKO myoblast cultures that Cdk5 activity was dramatically increased, although here through stabilization of p35. Thereby, depletion of the inhibitory nestin scaffold in the NesKO mice unleashes Cdk5 kinase activity by increasing the levels of its activator p35. As we have earlier shown that the generation of p25 is the key determinant to allow Cdk5-dependent differentiation to occur (de Thonel et al., 2010), and we could not detect consistent changes in the levels of p25 in NesKO myoblasts, it is perhaps not surprising that myoblast differentiation occurred normally in this setting. Although the differentiation-related Cdk5 activity is likely to be similar in both genotypes, the total Cdk5 activity was strongly upregulated in NesKO myoblasts. This is likely to affect several aspects of myoblast function, as Cdk5 activity is essential for myogenesis (Lazaro et al., 1997; Philpott et al., 1997). Correspondingly, in nestin-knockdown mice, the regulation of the Cdk5 activity associated with neuromuscular junctions was observed to be disrupted, leading to disturbed acetylcholine receptor clustering (Yang et al., 2011). Hence, our former and current results highlight that nestin, in different systems, has differential effects on Cdk5 signaling. Especially the effects on the p35 and p25 turnover seem to be highly dependent on the model system. Nonetheless, it is evident that nestin constitutes an important part of the Cdk5-restricting machinery in myoblasts. While Cdk5 is known to be essential for the course of myogenesis (Lazaro et al., 1997; Philpott et al., 1997), its direct targets (besides nestin) that drive myogenesis are not known. In fact, it has been suggested that either too little or too much Cdk5 activity can negatively impact myogenesis (Philpott et al., 1997), which opens up the possibility that Cdk5 acts at multiple levels of the myogenic process and has several important myogenic substrates. In future studies, it would be essential to understand the molecular roles of Cdk5 in both proliferating and differentiating myoblasts, and the distinction between the different activators during the course of differentiation, to understand the underlying signaling cascade that contributes to the NesKO phenotype.

IFs are crucial for organ integrity and healing, as has been established by the role of vimentin in wound healing (Cheng et al., 2016; Eckes et al., 2000). There are a number of mouse strains genetically deficient in different IFs that show dramatic regenerative muscle phenotypes, such as in the case of lamin A/C (Kubben et al.,

Journal of Cell Science (2017) 130, 2833-2842 doi:10.1242/jcs.202226

2011; Sullivan et al., 1999) and desmin (Li et al., 1996; Milner et al., 1996). These studies reinforce the view that IFs play an essential role in the maintenance of muscle architecture and integrity, and in muscle stem cell function. Knockout of less-well understood and less abundant IFs have also shown that these proteins have roles in muscle functioning. For example, synemin-null mice exhibit a mild regenerative muscle phenotype in baseline conditions, which under closer investigation revealed alterations in myoblast signaling, with consequences on muscle hypertrophy (García-Pelagio et al., 2015; Li et al., 2014). Similarly to our observations with the NesKO mice, synemin-null mice have an increased number of CLN in skeletal muscles (García-Pelagio et al., 2015; Li et al., 2014). These phenotypes show that both these highly specialized IFs play important roles in skeletal muscle biology, although both mouse models develop and function largely normally. Hence, our results are supportive of the well-recognized notion that IFs act as stress protectors in tissues (Toivola et al., 2010). Skeletal muscle is under constant physical and oxidative stress, which sets high requirements for a functional stress-response system. While IFs are direct targets of stress-induced phosphorylation, the removal of the IF networks, such as that of nestin, leaves the tissue with inapt cell signaling, thereby resulting in the tissue being more prone to injury-associated tissue dysfunction.

Nestin is an IF protein with highly specific expression patterns during both development and differentiation. The specific expression of nestin both in developing myofibers (in the present study) and in fully differentiated neuromuscular junctions (Yang et al., 2011) has been related to bidirectional signaling between nestin and Cdk5. The established paradigm of bidirectional signaling between nestin and Cdk5 paves the way towards a better understanding of the molecular causalities behind myodegenerative diseases.

MATERIALS AND METHODS

Animals

NesKO and WT mice in C57BL/6 background (Mohseni et al., 2011) were housed at the Central Animal Laboratory of the University of Turku on a 12-h-light–12-h-dark cycle and given standard rodent chow and water *ad libitum*.

For the *in vivo* regeneration study, 2-month-old male WT and NesKO mice were used. The mice were anesthetized with isoflurane and a transverse incision was made with a razor blade through the skin and half of the muscle thickness in the midbelly of the left tibialis anterior (TA) muscle. The skin was then sutured and the animals were allowed to move freely in their cages. The mice received pain relief in the form of buprenorfine (Temgesic, Reckitt Benckiser Healthcare) at 0.1 mg/kg body weight as an intraperitoneal injection at 0 and 8 h post operation as well as carprofen (Rimadyl, Pfizer Animal Health) at 5 mg/kg body weight as a subcutaneous injection at 0, 24 and 48 h post operation. The animals were euthanatized by carbon dioxide inhalation and cervical dislocation at indicated time points, and the TA muscles were dissected immediately and processed for paraffin embedding. The animal experiments were approved by the Finnish National Animal Experiment Board and performed according to The Finnish Act on Animal Experimentation (62/2006).

Histology

Tissues were fixed in 3% paraformaldehyde (PFA) in phosphate-buffered saline (PBS), dehydrated and embedded in paraffin; 2 µm thick sections were cut and collected on Superfrost Plus slides (Thermo Scientific). For tissue staining, the sections were de-paraffinized, rehydrated and stained with hematoxylin and eosin (H&E), or alternatively, tissue samples were blocked in Rodent Block M (Biocare Medical), incubated in primary antibody and species-specific BrightVision poly-HRP secondary antibody (ImmunoLogic) when performing HRP-based immunohistochemistry.

Picrosirius Red was used to stain collagen deposits and Fast Green FCF (Sigma-Aldrich) was used to counterstain muscle tissue in injured muscle sections. The sections were heated at 60°C for 45 min, hydrated and then incubated in a staining solution containing 0.1% Picrosirius Red and 0.1% FCF green in 1.2% picric acid solution for 60 min. Samples were washed in water, dehydrated and mounted.

Body composition measurement

The Echo-MRI body composition analyzer (EchoMRI LLC) was used to determine the lean and fat mass content of mice. This technology utilizes nuclear magnetic resonance to determine the amount of fat and lean mass of live conscious mice. Each mouse was measured twice.

Isolation of primary myoblasts and cell culture

Cells from adult mice were isolated as previously described (Danoviz and Yablonka-Reuveni, 2012). Briefly, the TA, extensor digitorum longus (EDL) and gastrocnemius muscles were isolated from adult mice and the muscles were digested in Dispase II (Stem Cell Technologies) and collagenase D (Roche Diagnostics), and satellite cells released by titration were collected by centrifugation (1000 ***g***, 10 min), and finally cultured on gelatin-coated dishes in standard growth medium for 3 days, and induced to differentiate by changing to differentiation medium. Standard growth medium for proliferating myoblast cultures consisted of Dulbecco's modified Eagle's medium (DMEM) (Sigma-Aldrich), 100 U/ml penicillin and 100 µg/ml streptomycin, 2 mM L-glutamine, 1 mM sodium pyruvate (Sigma-Aldrich), 20% fetal calf serum (Gibco), 10% horse serum (HyClone) and 1% chick embryo extract made in-house as previously described (Danoviz and Yablonka-Reuveni, 2012). Myoblasts were differentiated in 1% horse serum in DMEM with penicillin and streptomycin, 2 mM L-glutamine and 1 mM sodium pyruvate. Cells and myofibers were grown at 37°C and 5% CO_2 in humidified incubators.

Myofiber isolation and imaging

EDL muscles from both hind legs of 3-month-old male mice were used for myofiber preparation according to Keire et al. (2013). Briefly, muscles were dissected, digested in type I collagenase (Calbiochem) for 60 min and fibers were released by careful serial titration and washing. For confocal imaging purposes, myofibers were either immediately fixed in 3% PFA to assess the numbers of satellite cells, or grown individually in floating conditions in standard growth medium on horse serum-coated tissue culture dishes for 72 h to allow satellite cell activation on top of the myofibers, until they were fixed in PFA and immunostained for myogenic markers.

For continuous phase-contrast imaging with Cell-IQ imaging platform (CM Technologies), isolated myofibers were allowed to attach to the bottom of Matrigel (BD Biosciences)-coated cell culture plates for 48 h. Subsequently, imaging was performed with a CO_2 supply at 37°C in standard growth medium for an additional 96 h to study the proliferation and expansion of emerging satellite cells (Fig. S4). A representative video of the myofiber culture is available as Movie 1.

Immunocytochemistry

Cells were washed in PBS after fixation, permeabilized with 0.5% Triton-X 100 for 10 min and blocked in 1% bovine serum albumin (BSA) in PBS solution for 1 h. Primary antibody (Table S1) was added at the appropriate antibody-specific concentration and incubated for 2 h. Coverslips were washed three times in PBS before addition of secondary antibodies (species-specific Alexa Fluor 488 or 555, Invitrogen). After 1 h of incubation in secondary antibody, samples were again washed in PBS, and mounted in ProLong Gold reagent with 4′,6-diamidino-2-phenylindole (DAPI) (Life Technologies). Myofibers were immunolabeled similarly to cells, with some modifications: floating individual myofibers were blocked in 5% BSA in PBS for 2 h and incubated in primary antibody solution for two more hours. Finally, myofibers were mounted on coverslips in ProLong Gold mounting agent with DAPI (Life Technologies).

Microscopy and image analysis

An LSM 780 confocal microscope (Zeiss) was used for imaging of cells and myofibers, and ZEN 2012 (Zeiss), ImageJ or BioimageXD software were used to process images. A Pannoramic 250 Slide Scanner (3D Histech) was used for brightfield imaging of histological samples, and CaseViewer and Pannoramic Viewer (3D Histech) software were used to export images, as well as for manual quantification of injury areas and myofiber size in muscle sections. The regenerating muscle area (injury area over total muscle area) was calculated from six separate histological sections per mouse, of which an average value was calculated for each mouse. The regenerating muscle area was defined by the presence of myofibers containing CLN residing in immediate vicinity of each other.

To quantify satellite cell numbers from live Cell-IQ microscopy experiments, nine image fields per genotype from three independent experiments were processed with similar settings using Cell-IQ Analyser software (CM Technologies) to quantify the number of cells emerging from the attached myofibers. The area occupied by myofibers in each image was comparable in all samples (3–8% of the total pixel area). The number of cells per field was plotted against time. To estimate satellite cell cycle length, manual cell lineage tracking was performed with the Fiji plugin TrackMate from the Cell-IQ imaging data. Cells were tracked for four generations corresponding to approximately the first 40 h of imaging. The time between two cell divisions was calculated from the data and plotted.

To enhance the visibility of the collagen in the Picrosirius Red and Fast Green FCF staining the red color was extracted from the images using color deconvolution with the setting 'Feulgen Light Green' in Fiji/ImageJ (Schindelin et al., 2012). The resulting image was then converted to a binary image using Fiji.

Western blotting

Cells were lysed in Laemmli lysis buffer, separated on acrylamide gels using SDS-PAGE and transferred to polyvinylidene fluoride membranes (BioRad). After blocking in milk, membranes were incubated in primary antibody overnight. All used antibodies are tabulated in Table S1. After washing, species-specific horseradish peroxidase (HRP)-conjugated secondary antibodies were applied to the membranes, which were washed after incubation and detected using enhanced chemiluminiscence reagent (GE Healthcare) on X-ray films (Fujifilm).

Kinase assay

Primary myoblasts from 3-month-old male mice were induced to differentiate for 24 h, lysed 30 min in lysis buffer [50 mM Tris-HCl pH 8.0, 150 mM NaCl, 1% Nonidet P-40, 0.5% sodium deoxycholate, 0.05% SDS, 5 mM EDTA, 5 mM EGTA, Complete protease inhibitor cocktail (Roche Diagnostics), PhosSTOP phosphatase inhibitor cocktail (Roche Diagnostics)] and centrifuged (15,000 ***g*** for 10 min). The supernatant was pre-cleared with Sepharose G beads (GE Healthcare) and incubated with anti-Cdk5 antibody for 1 h. Protein G–Sepharose was added and samples were incubated under rotation for 2.5 h. Samples were washed once with lysis buffer and two times with kinase reaction buffer (50 mM HEPES pH 7.2, 0.1 mM EDTA, 0.1 mM EGTA, 5 mM $MgCl_2$). A mixture of ATP and 3 µCi [γ-^{32}P]ATP was added to the beads to a final concentration of 100 µM. Histone H1 (Sigma-Aldrich) was phosphorylated in a kinase reaction for 30 min at 30°C, and lysed in Laemmli lysis buffer. The samples were run on 12.5% SDS-PAGE and stained with Coomassie Brilliant Blue. After drying, the ^{32}P-labeled histone was visualized on X-ray film (Fujifilm).

Statistics

GraphPad Prism 6 (GraphPad Software) was used to analyze statistical significance by using an unpaired Student's *t*-test, unpaired Student's *t*-test with Welch's correction or Mann–Whitney test when samples were not normally distributed (D'Agostino-Pearson omnibus normality test or Shapiro–Wilk normality test) depending on the experimental setup. All results are presented as mean±s.e.m. $P<0.05$ is considered significant and marked with asterisks (*$P<0.05$, **$P<0.005$, ***$P<0.001$, ****$P<0.0001$); n.s. stands for not statistically significant ($P>0.05$). $n\geq3$ in all the experiments.

Acknowledgements

Sinikka Collanus is acknowledged for assistance in histological applications. Turku Bioimaging and Cell Imaging Core at Turku Centre for Biotechnology are acknowledged for assistance with microscopy.

Competing interests

The authors declare no competing or financial interests.

Author contributions

Conceptualization: J.L., E.T., J.E.E.; Formal analysis: J.L., E.T.; Investigation: J.L., E.T., J.G., H.K.; Resources: A.N., P.T.; Writing - original draft: J.L., E.T., J.E.E.; Writing - review & editing: J.L., E.T., J.E.E.; Supervision: P.T., J.E.E.; Funding acquisition: P.T., J.E.E.

Funding

J.E.E. was supported by the Sigrid Jusélius Foundation (Sigrid Juséliuksen säätiö), the Academy of Finland (Suomen Akatemia), the Finnish Cancer Foundations, the Magnus Ehrnrooth foundation (Magnus Ehrnroothin säätiö), the Foundation 'Konung Gustaf V:s och Drottning Victorias Frimurarestiftelse', and the Endowment of the Åbo Akademi University; J.L. was supported by the Turku Graduate School of Biomedical Sciences; J.G. was supported by Turku Doctoral Network in Molecular Biosciences, the K. Albin Johansson Foundation, the Magnus Ehrnrooth Foundation, the Foundation 'Medicinska Understödsföreningen Liv & Hälsa', the Foundation 'Finsk-Norska Medicinska Stiftelsen', the Swedish Cultural Foundation, and the Waldemar von Frenckell Foundation; P.T. was supported by the Finnish Medical Foundation (Suomen Lääketieteen Säätiö) and the Academy of Finland (Suomen Akatemia).

Supplementary information

Supplementary information available online at
http://jcs.biologists.org/lookup/doi/10.1242/jcs.202226.supplemental

References

Cadot, B., Gache, V. and Gomes, E. R. (2015). Moving and positioning the nucleus in skeletal muscle – one step at a time. *Nucleus* **6**, 373-381.

Carboni, N., Mateddu, A., Marrosu, G., Cocco, E. and Marrosu, M. G. (2013). Genetic and clinical characteristics of skeletal and cardiac muscle in patients with lamin A/C gene mutations. *Muscle Nerve.* **48**, 161-170.

Carlsson, L., Li, Z., Paulin, D. and Thornell, L. E. (1999). Nestin is expressed during development and in myotendinous and neuromuscular junctions in wild type and desmin knock-out mice. *Exp. Cell Res.* **251**, 213-223.

Cheng, F., Shen, Y., Mohanasundaram, P., Lindström, M., Ivaska, J., Ny, T. and Eriksson, J. E. (2016). Vimentin coordinates fibroblast proliferation and keratinocyte differentiation in wound healing via TGF-β–Slug signaling. *Proc. Natl. Acad. Sci. USA* **113**, E4320-E4327.

Ciciliot, S. and Schiaffino, S. (2010). Regeneration of mammalian skeletal muscle: basic mechanisms and clinical implications. *Curr. Pharm. Des.* **16**, 906-914.

Contreras-Vallejos, E., Utreras, E. and Gonzalez-Billault, C. (2012). Going out of the brain: non-nervous system physiological and pathological functions of Cdk5. *Cell. Signal.* **24**, 44-52.

Daniel, C., Albrecht, H., Lüdke, A. and Hugo, C. (2008). Nestin expression in repopulating mesangial cells promotes their proliferation. *Lab. Investig. J. Tech. Methods Pathol.* **88**, 387-397.

Danoviz, M. E. and Yablonka-Reuveni, Z. (2012). Skeletal muscle satellite cells: background and methods for isolation and analysis in a primary culture system. *Methods Mol. Biol. Clifton NJ* **798**, 21-52.

Day, K., Shefer, G., Richardson, J. B., Enikolopov, G. and Yablonka-Reuveni, Z. (2007). Nestin-GFP reporter expression defines the quiescent state of skeletal muscle satellite cells. *Dev. Biol.* **304**, 246-259.

de Thonel, A., Ferraris, S. E., Pallari, H.-M., Imanishi, S. Y., Kochin, V., Hosokawa, T., Hisanaga, S., Sahlgren, C. and Eriksson, J. E. (2010). Protein kinase Czeta regulates Cdk5/p25 signaling during myogenesis. *Mol. Biol. Cell* **21**, 1423-1434.

Eckes, B., Colucci-Guyon, E., Smola, H., Nodder, S., Babinet, C., Krieg, T. and Martin, P. (2000). Impaired wound healing in embryonic and adult mice lacking vimentin. *J. Cell Sci.* **113**, 2455-2462.

Folker, E. S. and Baylies, M. K. (2013). Nuclear positioning in muscle development and disease. *Front. Physiol.* **4**, 363.

García-Pelagio, K. P., Muriel, J., O'Neill, A., Desmond, P. F., Lovering, R. M., Lund, L., Bond, M. and Bloch, R. J. (2015). Myopathic changes in murine skeletal muscle lacking synemin. *Am. J. Physiol. Cell Physiol.* **308**, C448-C462.

Goldfarb, L. G. and Dalakas, M. C. (2009). Tragedy in a heartbeat: malfunctioning desmin causes skeletal and cardiac muscle disease. *J. Clin. Invest.* **119**, 1806-1813.
Gruenbaum, Y. and Aebi, U. (2014). Intermediate filaments: a dynamic network that controls cell mechanics. *F1000Prime Rep.* **6**, 54.
Hockfield, S. and McKay, R. D. (1985). Identification of major cell classes in the developing mammalian nervous system. *J. Neurosci. Off. J. Soc. Neurosci.* **5**, 3310-3328.
Hyder, C. L., Isoniemi, K. O., Torvaldson, E. S. and Eriksson, J. E. (2011). Insights into intermediate filament regulation from development to ageing. *J. Cell Sci.* **124**, 1363-1372.
Kachinsky, A. M., Dominov, J. A. and Miller, J. B. (1995). Intermediate filaments in cardiac myogenesis: nestin in the developing mouse heart. *J. Histochem. Cytochem. Off. J. Histochem. Soc.* **43**, 843-847.
Keire, P., Shearer, A., Shefer, G. and Yablonka-Reuveni, Z. (2013). Isolation and culture of skeletal muscle myofibers as a means to analyze satellite cells. *Methods Mol. Biol. Clifton NJ* **946**, 431-468.
Kubben, N., Voncken, J. W., Konings, G., van Weeghel, M., van den Hoogenhof, M. M., Gijbels, M., van Erk, A., Schoonderwoerd, K., van den Bosch, B., Dahlmans, V. et al. (2011). Post-natal myogenic and adipogenic developmental: defects and metabolic impairment upon loss of A-type lamins. *Nucl. Austin Tex* **2**, 195-207.
Lazaro, J. B., Kitzmann, M., Poul, M. A., Vandromme, M., Lamb, N. J. and Fernandez, A. (1997). Cyclin dependent kinase 5, cdk5, is a positive regulator of myogenesis in mouse C2 cells. *J. Cell Sci.* **110**, 1251-1260.
Li, Z., Colucci-Guyon, E., Pinçon-Raymond, M., Mericskay, M., Pournin, S., Paulin, D. and Babinet, C. (1996). Cardiovascular lesions and skeletal myopathy in mice lacking desmin. *Dev. Biol.* **175**, 362-366.
Li, Z., Parlakian, A., Coletti, D., Alonso-Martin, S., Hourdé, C., Joanne, P., Gao-Li, J., Blanc, J., Ferry, A., Paulin, D. et al. (2014). Synemin acts as a regulator of signalling molecules during skeletal muscle hypertrophy. *J. Cell Sci.* **127**, 4589-4601.
Li, J., Wang, R., Yang, L., Wu, Q., Wang, Q., Nie, Z., Yu, Y., Ma, J. and Pan, Q. (2015). Knockdown of Nestin inhibits proliferation and migration of colorectal cancer cells. *Int. J. Clin. Exp. Pathol.* **8**, 6377-6386.
Milner, D. J., Weitzer, G., Tran, D., Bradley, A. and Capetanaki, Y. (1996). Disruption of muscle architecture and myocardial degeneration in mice lacking desmin. *J. Cell Biol.* **134**, 1255-1270.
Milner, D. J., Mavroidis, M., Weisleder, N. and Capetanaki, Y. (2000). Desmin cytoskeleton linked to muscle mitochondrial distribution and respiratory Function. *J. Cell Biol.* **150**, 1283-1298.
Mohseni, P., Sung, H.-K., Murphy, A. J., Laliberte, C. L., Pallari, H.-M., Henkelman, M., Georgiou, J., Xie, G., Quaggin, S. E., Thorner, P. S. et al. (2011). Nestin is not essential for development of the CNS but required for dispersion of acetylcholine receptor clusters at the area of neuromuscular junctions. *J. Neurosci. Off. J. Soc. Neurosci.* **31**, 11547-11552.
Pallari, H.-M., Lindqvist, J., Torvaldson, E., Ferraris, S. E., He, T., Sahlgren, C. and Eriksson, J. E. (2011). Nestin as a regulator of Cdk5 in differentiating myoblasts. *Mol. Biol. Cell* **22**, 1539-1549.
Philpott, A., Porro, E. B., Kirschner, M. W. and Tsai, L. H. (1997). The role of cyclin-dependent kinase 5 and a novel regulatory subunit in regulating muscle differentiation and patterning. *Genes Dev.* **11**, 1409-1421.
Sahlgren, C. M., Mikhailov, A., Vaittinen, S., Pallari, H.-M., Kalimo, H., Pant, H. C. and Eriksson, J. E. (2003). Cdk5 regulates the organization of Nestin and its association with p35. *Mol. Cell. Biol.* **23**, 5090-5106.
Sahlgren, C. M., Pallari, H.-M., He, T., Chou, Y.-H., Goldman, R. D. and Eriksson, J. E. (2006). A nestin scaffold links Cdk5/p35 signaling to oxidant-induced cell death. *EMBO J.* **25**, 4808-4819.
Schindelin, J., Arganda-Carreras, I., Frise, E., Kaynig, V., Longair, M., Pietzsch, T., Preibisch, S., Rueden, C., Saalfeld, S., Schmid, B. et al. (2012). Fiji: an open-source platform for biological-image analysis. *Nat. Methods* **9**, 676-682.
Sejersen, T. and Lendahl, U. (1993). Transient expression of the intermediate filament nestin during skeletal muscle development. *J. Cell Sci.* **106**, 1291-1300.
Shah, K. and Lahiri, D. K. (2014). Cdk5 activity in the brain - multiple paths of regulation. *J. Cell Sci.* **127**, 2391-2400.
Shi, X. and Garry, D. J. (2006). Muscle stem cells in development, regeneration, and disease. *Genes Dev.* **20**, 1692-1708.
Sjöberg, G., Edström, L., Lendahl, U. and Sejersen, T. (1994a). Myofibers from Duchenne/Becker muscular dystrophy and myositis express the intermediate filament nestin. *J. Neuropathol. Exp. Neurol.* 53, 416-423.
Sjöberg, G., Jiang, W.-Q., Ringertz, N. R., Lendahl, U. and Sejersen, T. (1994b). Colocalization of nestin and vimentin/desmin in skeletal muscle cells demonstrated by three-dimensional fluorescence digital imaging microscopy. *Exp. Cell Res.* **214**, 447-458.
Steinert, P. M., Chou, Y. H., Prahlad, V., Parry, D. A., Marekov, L. N., Wu, K. C., Jang, S. I. and Goldman, R. D. (1999). A high molecular weight intermediate filament-associated protein in BHK-21 cells is nestin, a type VI intermediate filament protein. Limited co-assembly in vitro to form heteropolymers with type III vimentin and type IV alpha-internexin. *J. Biol. Chem.* **274**, 9881-9890.
Stone, M. R., O'Neill, A., Lovering, R. M., Strong, J., Resneck, W. G., Reed, P. W., Toivola, D. M., Ursitti, J. A., Omary, M. B. and Bloch, R. J. (2007). Absence of keratin 19 in mice causes skeletal myopathy with mitochondrial and sarcolemmal reorganization. *J. Cell Sci.* **120**, 3999-4008.
Sullivan, T., Escalante-Alcalde, D., Bhatt, H., Anver, M., Bhat, N., Nagashima, K., Stewart, C. L. and Burke, B. (1999). Loss of A-type lamin expression compromises nuclear envelope integrity leading to muscular dystrophy. *J. Cell Biol.* **147**, 913-920.
Tampaki, E. C., Nakopoulou, L., Tampakis, A., Kontzoglou, K., Weber, W. P. and Kouraklis, G. (2014). Nestin involvement in tissue injury and cancer–a potential tumor marker? *Cell. Oncol. Dordr.* **37**, 305-315.
Toivola, D. M., Strnad, P., Habtezion, A. and Omary, M. B. (2010). Intermediate filaments take the heat as stress proteins. *Trends Cell Biol.* **20**, 79-91.
Tschaharganeh, D. F., Xue, W., Calvisi, D. F., Evert, M., Michurina, T. V., Dow, L. E., Banito, A., Katz, S. F., Kastenhuber, E. R., Weissmueller, S. et al. (2014). p53-dependent nestin regulation links tumor suppression to cellular plasticity in liver cancer. *Cell* **158**, 579-592.
Vaittinen, S., Lukka, R., Sahlgren, C., Rantanen, J., Hurme, T., Lendahl, U., Eriksson, J. E. and Kalimo, H. (1999). Specific and innervation-regulated expression of the intermediate filament protein nestin at neuromuscular and myotendinous junctions in skeletal muscle. *Am. J. Pathol.* **154**, 591-600.
Vaittinen, S., Lukka, R., Sahlgren, C., Hurme, T., Rantanen, J., Lendahl, U., Eriksson, J. E. and Kalimo, H. (2001). The expression of intermediate filament protein nestin as related to vimentin and desmin in regenerating skeletal muscle. *J. Neuropathol. Exp. Neurol.* **60**, 588-597.
Wiese, C., Rolletschek, A., Kania, G., Blyszczuk, P., Tarasov, K. V., Tarasova, Y., Wersto, R. P., Boheler, K. R. and Wobus, A. M. (2004). Nestin expression–a property of multi-lineage progenitor cells? *Cell. Mol. Life Sci. CMLS* **61**, 2510-2522.
Worman, H. J., Fong, L. G., Muchir, A. and Young, S. G. (2009). Laminopathies and the long strange trip from basic cell biology to therapy. *J. Clin. Invest.* **119**, 1825-1836.
Wroblewski, J., Engström, M., Edwall-Arvidsson, C., Sjöberg, G., Sejersen, T. and Lendahl, U. (1997). Distribution of nestin in the developing mouse limb bud in vivo and in micro-mass cultures of cells isolated from limb buds. *Differ. Res. Biol. Divers.* **61**, 151-159.
Yang, J., Dominguez, B., de Winter, F., Gould, T. W., Eriksson, J. E. and Lee, K.-F. (2011). Nestin negatively regulates postsynaptic differentiation of the neuromuscular synapse. *Nat. Neurosci.* **14**, 324-330.
Yin, H., Price, F. and Rudnicki, M. A. (2013). Satellite cells and the muscle stem cell niche. *Physiol. Rev.* **93**, 23-67.
Zhao, Z., Lu, P., Zhang, H., Xu, H., Gao, N., Li, M. and Liu, C. (2014). Nestin positively regulates the Wnt/β-catenin pathway and the proliferation, survival and invasiveness of breast cancer stem cells. *Breast Cancer Res. BCR* **16**, 408.